Spheromak injection into a tokamak*

M. R. Brown[†,a)] and P. M. Bellan
California Institute of Technology, Pasadena, California 91125

(Received 13 November 1989; accepted 21 February 1990)

Recent results from the Caltech spheromak injection experiment [to appear in Phys. Rev. Lett.] are reported. First, current drive by spheromak injection into the ENCORE tokamak as a result of the process of magnetic helicity injection is observed. An initial 30% increase in plasma current is observed followed by a drop by a factor of 3 because of sudden plasma cooling. Second, spheromak injection results in an increase of tokamak central density by a factor of 6. The high-current/high-density discharge is terminated by a sharp peaking of the density profile followed by an interchange instability. In a second experiment, the spheromak is injected into the magnetized toroidal vacuum vessel (with no tokamak plasma) fitted with magnetic probe arrays. An $m = 1$ (nonaxisymmetric) magnetic structure forms in the vessel after the spheromak undergoes a double tilt; once in the cylindrical entrance between gun and tokamak, then again in the tokamak vessel. In the absence of net toroidal flux, the structure develops a helical pitch (the sense of pitch depends on the helicity sign). Experiments with a number of refractory metal electrode coatings have shown that tungsten and chrome coatings provide some improvement in spheromak parameters. Design details of a larger, higher-current spheromak gun with a new accelerator section are also discussed.

I. INTRODUCTION

A spheromak is a magnetized plasma configuration of the "compact toroid" class (no material linking the hole in the torus). Because spheromaks have a relatively high magnetic helicity content and high plasma density, spheromak injection into tokamaks has been proposed as a means of tokamak current drive[1] and refueling.[2,3] Magnetic helicity[4] is a measure of linked magnetic flux and is closely related to field-aligned current. It is postulated that since magnetic helicity is a scalar, additive, nearly conserved quantity in resistive magnetohydrodynamics (MHD) (even in the presence of turbulent tearing[5]), the merging of a spheromak and tokamak with the same sign of helicity will yield a tokamak of higher helicity content (which, for a tokamak, corresponds to a higher toroidal current).

Spheromaks have been successfully injected into the Caltech ENCORE tokamak ($R = 0.38$ m, $a = 0.12$ m, $I_p = 2$ kA, and $B_{tor} = 700$ G) in order to add helicity and density.[6] Current drive in the tokamak was observed *only when both spheromak and tokamak had the same sign of helicity* [the helicity sign is defined as positive (right handed) if current flows parallel to the magnetic field and negative (left handed) if antiparallel]. Spheromak injection also increased the tokamak central density by a factor of 6 (from 1 to 6×10^{18} m^{-3}). The process of helicity conservation has previously been demonstrated in detail in the CTX spheromak,[7] wherein a coaxial magnetized plasma gun injected helicity into a simply connected flux conserver. The present results indicate that the processes of helicity injection and conservation are applicable to tokamak plasmas.

A related issue is the equilibrium configuration of spheromaks in magnetized toroidal flux conservers. The equilibrium magnetic structure of spheromaks in cylindrical flux conservers has been studied experimentally[8] and theoretically.[9,10] In addition, theoretical studies have been performed on spheromaks in infinite conducting cylinders.[5,11] Spheromaks have been injected into the ENCORE toroidal vacuum vessel (with no tokamak plasma) and a twisted, $m = 1$ (nonaxisymmetric) magnetic configuration is formed after undergoing a double tilt; once in the cylindrical entrance region, then again in the tokamak vessel. Using a fit of the data to a simple model, we are able to calculate the total helicity content and magnetic energy of our injected spheromaks.

Finally, it is important for spheromak injection that high-Z impurities from the gun electrodes be minimized; impurities are a deleterious addition to the tokamak and impurities reduce the magnetic lifetime of spheromaks injected into the toroidal chamber. We have experimented with a number of refractory metal coatings on our center electrode (bare steel, copper, nickel, chromium, rhodium, and tungsten coatings) in order to improve spheromak parameters.

II. SPHEROMAK INJECTION

The Caltech spheromak is formed with a coaxial magnetized plasma gun (Fig. 1) ($I_{gun} = 80$ kA, $\Phi_{gun} = 0.4$ m Wb, and peak $B_{sph} = 5$ kG) similar in design to those used by Alfvén *et al.*[12] We are able to generate spheromaks and tokamaks of either helicity sign. We change the sign of the tokamak helicity by reversing the direction of the toroidal field (while maintaining the direction of the plasma current) and the sign of spheromak helicity is reversed by changing the direction of the coaxial gun magnetization (while maintaining the polarity of the gun voltage). In Figs. 2(a) and 2(c), we show the time history of the tokamak plasma current with injection of a spheromak into a tokamak discharge of

*Paper 1I7, Bull. Am. Phys. Soc. **34**, 1913 (1989).
[†] Invited speaker.
[a)] United States Department of Energy Fusion Energy Postdoctoral Research Fellow.

 0899-8221/90/061306-05$02.00

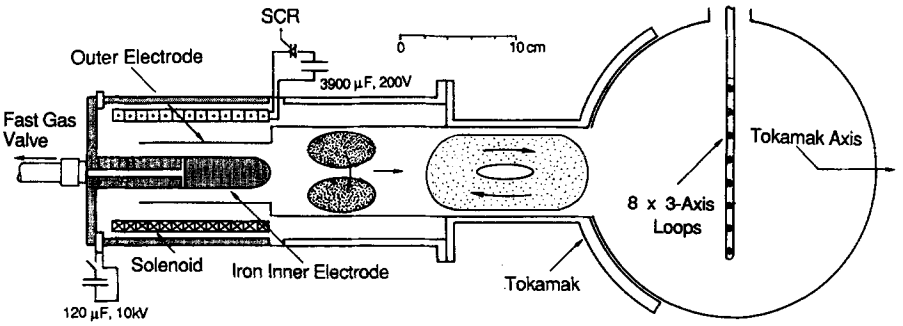

FIG. 1. Schematic of experimental setup showing topology of an injected spheromak.

the same sign (both left handed and both right handed, respectively), while in Figs. 2(b) and 2(d) we show the effect of injecting a spheromak into a tokamak of opposite helicity sign (left into right and right into left). Note that when helicities are of the same (opposite) sign an increase (decrease) in tokamak current is observed (the less pronounced decrease in current in the right-into-left case shown in Fig. 2(d) is due to permanent magnetization of our electrode, which makes it difficult to generate right-handed spheromaks). The initial increase (decrease) in current is also accompanied by a sharp decrease (increase) in loop voltage. It is useful to view the spheromak as a tightly coiled spring (high helicity content) and the tokamak as a loosely coiled spring (low helicity content). If the tightly coiled spring could be inserted into the loosely coiled one (reconnection) and if both springs had the same pitch, then as the tight spring uncoiled the loose spring would become more tightly coiled.

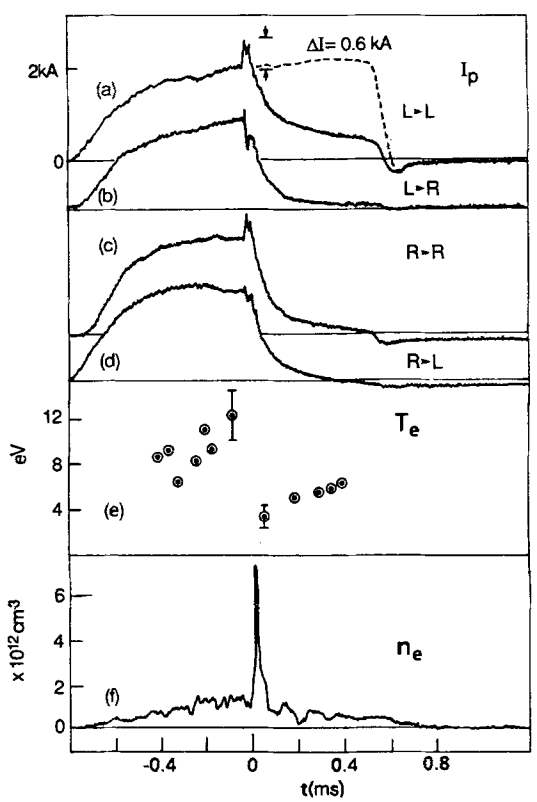

FIG. 2. Time histories of the tokamak discharge ($B_{tor} = 700$ G) with spheromak injection ($I_{gun} = 80$ kA, $\Phi_{gun} = 0.4$ m Wb), time scale relative to injection: (a) I_p with a left-handed spheromak injected into a left-handed tokamak (dashed line is normal discharge without spheromak injection); (b) left into right; (c) right into right; (d) right into left; (e) electron temperature; and (f) density traces from Langmuir probe measurements.

The helicity content of the injected spheromak can be estimated a number of ways. First, the formal definition ($K = \int A \cdot B \, d^3x$) can be approximated by $K_{sph} \cong \alpha \Phi_{tor} \Phi_{pol}$, where α is a constant of order unity. For the case of two separate, discrete linked fluxes[4] $\alpha = 2$; for the case of an axisymmetric spheromak in a cylindrical flux conserver[13] α is close to unity. The helicity content of the spheromak that ultimately moves into the tokamak is estimated from measurements performed on the spheromak in the tokamak vessel without tokamak plasma (see, for example, the data presented in Fig. 5). We can therefore estimate $K_{sph} \cong \Phi_{tor} \Phi_{pol} \cong (B_{ave} \pi r^2/2) \quad (B_{ave} \pi L r/8) \cong B^2_{ave} \pi^2 L r^3/16$, where Φ_{tor} is the spheromak toroidal flux that passes through one-half of the tokamak minor cross section and Φ_{pol} is the flux that passes through the spheromak magnetic axis [which we assume is an ellipse of minor radius $r/2$ and major radius $L/4$ in the center of the spheromak (see Fig. 3)]. In this estimate, B_{ave} is the volume-averaged magnetic field measured in the spheromak equilibrium, L is its length, and r is the radius of the cylindrical flux conserver (the tokamak minor radius in this case). From extensive magnetic probe measurements performed in the tokamak vacuum vessel we typically find $B_{ave} \cong 200$ G, $r = 0.12$ m, and $L \cong 4r$ so that $K_{sph} = 2 \times 10^{-7}$ Wb^2. Equivalently, we may also make this estimate by noting[7] that the energy per unit helicity of the spheromak equilibrium, $2\mu_0 W_{mag}/K_{sph} = \lambda_{eq}$ [where $W_{mag} = (B^2_{ave}/2\mu_0)\pi r^2 L$ is the spheromak magnetic energy and λ_{eq} is the eigenvalue of the equation of the force-free state, $\nabla \times B = \lambda_{eq} B$]. For an axisymmetric spheromak in a cylindrical flux conserver we have[10] $\lambda_{eq} = (k_z^2 + k_r^2)^{1/2}$ where $k_z = \pi/L$ and $k_r = 3.83/r$ (from a more careful fit of the data to a simple model, we obtain roughly the same value

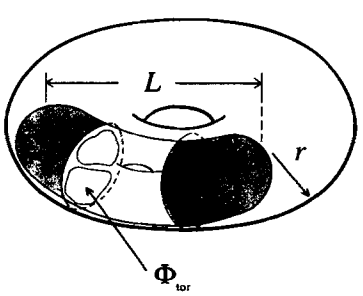

FIG. 3. Schematic showing dimensions used for spheromak helicity estimates.

for λ_{eq}). From the measurements discussed above, we find $\lambda_{eq} = 32\ m^{-1}$ from which we obtain roughly the same result $K_{sph} = 3\times10^{-7}\ Wb^2$. Third, we may estimate the helicity content of the spheromak by first noting that helicity is generated by the coaxial magnetized plasma gun at a rate[7] $\dot{K} = 2V_{gun}\Phi_{gun}$, where V_{gun} is the voltage that develops between inner and outer electrodes. Note that V_{gun} is determined by gun impedance and is usually *significantly* less than the voltage on the capacitor bank. We find that $K_{initial} \cong \int 2V_{gun}\Phi_{gun}\,dt \cong 4\times10^{-6}\ Wb^2$ for typical values of $V_{gun} = 1\ kV$, $\Phi_{gun} = 0.4\ m\ Wb$, and the duration the voltage is applied, $\Delta t \cong 5\ \mu sec$. We make the further observations that (1) the magnetic e-folding decay time of our spheromaks is $10\ \mu sec$ so that the helicity decay time, $\tau_K \cong \tau_R/2$, is about $5\ \mu sec$ and that (2) the velocity of our spheromaks is about $3\ cm/\mu sec$. We may infer, then, that the initial helicity content of our spheromak decays about two e-folding times while traversing the 30 cm between gun and tokamak (i.e., $K_{sph} = K_{initial}e^{-t/\tau_K}$). We find by this calculation that $K_{sph} = 5\times10^{-7}\ Wb^2$, consistent with the other two methods. Finally, the tokamak helicity can be estimated by $K_{tok} \cong \Phi_{tor}\Phi_{pol}$, so we obtain

$$\Delta K_{tok} \cong \mu_0 \pi B_{tor}\Delta I_p a^2 R/2 \cong 4.5\times10^{-7}\ Wb^2$$

for $\Delta I_p = 600$ A and $B_{tor} = 700$ G. We conclude that the increase in tokamak helicity is consistent with the helicity of the injected spheromak.

The injection of the cold, dense spheromak ($n_e \cong 10^{21}\ m^{-3}$, $T_e \cong 5$ eV) into the warm, tenuous tokamak plasma causes a sudden cooling [Fig. 2(e)]. The cooling (in conjunction with the disruptive interchange instability described below) causes a gradual drop in plasma current by a factor of 3. The calculated L/R decay time of the plasma current due to cooling is $\cong 70\ \mu sec$ (for $L_{tok} \cong 0.5\ \mu H$ and $R_{tok} \cong 7\ m\ \Omega$ assuming Spitzer resistivity with $Z = 2$ and $T_e = 4$ eV), which is about the observed value. Spheromak injection also raises the tokamak central density by a factor of 6 [Fig. 2(f)], but the high-density discharge is short lived. Measurement of the radial density profile (with a Langmuir probe array one-quarter of the tokamak circumference away from the injection port) shows that the rapid peaking of the profile is followed by a hollowing, suggestive of a pressure gradient induced interchange instability. In Fig. 4, the time history of the radial density profile is depicted beginning just before the profile peaks (about $50\ \mu sec$ after injection of the spheromak). Note that the peaking is followed by rapid drop in central density and a hollowing of the profile (at $54\ \mu sec$). Finally, the profile returns to a less peaked configuration about $60\ \mu sec$ after injection.

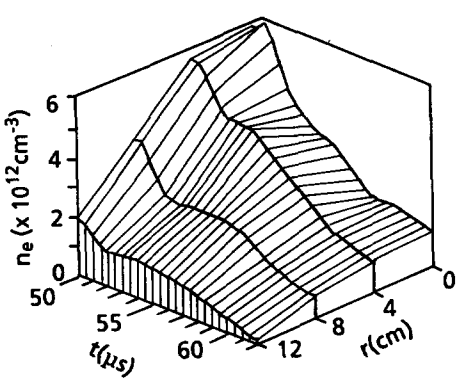

FIG. 4. Tokamak radial density profile upon injection of a spheromak showing peaking and hollowing indicative of a pressure gradient induced interchange instability.

III. MAGNETIC PROBE ARRAYS

In a second series of experiments, the spheromak is injected into the magnetized toroidal vacuum vessel (without tokamak plasma) fitted with arrays of magnetic probes. A linear array of 24 discrete magnetic pickup loops measures all components of $\tilde{\mathbf{B}}$ simultaneously at eight locations across the tokamak minor diameter directly in front of the gun (see Fig. 1). In addition, loops arranged in two quartz jacketed crosses have been used either to measure one component of the spheromak magnetic field (toroidal or poloidal) at three radii and four poloidal points (a total of 12 locations) at two toroidal locations or both toroidal and poloidal components in either the right or the left cross (see Fig. 5). An eight-sided array has also been used to study the toroidal component of the magnetic field in more detail in the poloidal cross section. These measurements show that the spheromak (i) is initially generated with its axis directed away from the gun; then (ii) tilts while in the cylindrical entrance region and moves into the tokamak vessel with its axis aligned in the

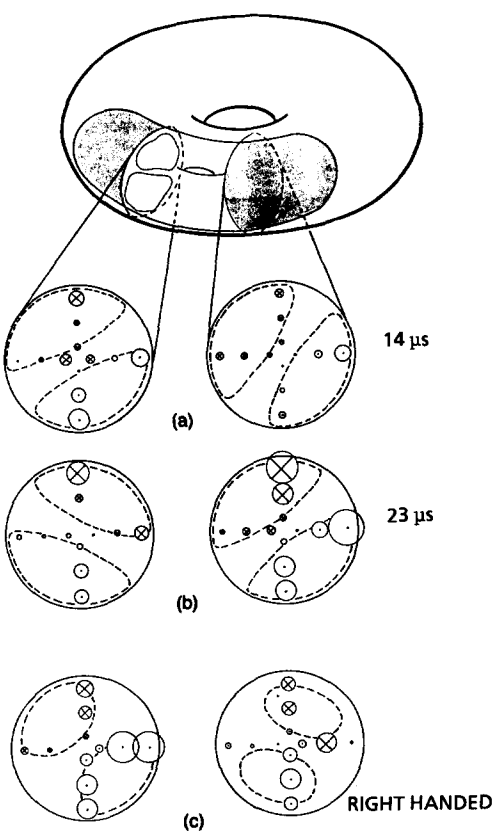

FIG. 5. Data from a cross-shaped probe array (no tokamak plasma). (a) A left-handed spheromak with $m = 1$ shape in the toroidal vessel ($14\ \mu sec$) develops (b) a 60° helical twist ($23\ \mu sec$); (c) a right-handed spheromak develops a twist in the opposite sense. The largest circles represent about 300 G.

direction *opposite* the tokamak's toroidal field; then finally (iii), while in the tokamak vacuum vessel, tilts again, directing its axis inward toward the axis of the tokamak. There is also evidence of a vertical drift of the spheromak in the $\mathbf{J}_{pol} \times \mathbf{B}_{tor}$ direction (where $\mathbf{J}_{pol}$ is the current that threads the center of the spheromak). The ultimate configuration is that of an $m = 1$ (nonaxisymmetric) magnetic equilibrium. Measurements in the tokamak poloidal cross section at two toroidal locations (to the left and right sides of the spheromak entrance port) show that the spheromak shifts horizontally in the direction opposite that of the applied dc toroidal field. In the absence of toroidal flux the $m = 1$ spheromak develops a helical twist and some deviations from $m = 1$ symmetry on the inboard side of the tokamak as a result of toroidal effects. The data is well described by a pressureless, force-free model equilibrium solved in an infinite, perfectly conducting cylinder.[11] Deviations from the fit appear to be due to toroidal effects, finite pressure,[14] and a nonuniform J/B profile.[15] Calculations based on the data fitted to the model provide better estimates of the total helicity content and magnetic energy of injected spheromaks.

As an example of our magnetic data, results from the cross-shaped probes are presented in Fig. 5. The left side of each figure is the outboard side of the tokamak, the right is the inboard (the spheromak enters from the left). The diameter of the circles is proportional to the measured magnetic field while a dot (cross) represents a right-going (left-going) magnetic field (the largest circles represent about 300 G). Data of one sign of toroidal flux are encircled by a contour of constant poloidal flux ($\Phi_{pol} = \text{const}$, computed from a model fit). In these discharges there is no net applied tokamak toroidal flux. Note that the equilibrium [a left-handed spheromak in Figs. 5(a) and 5(b)] has an $m = 1$ symmetry and both left and right arrays have a similar magnetic signature at 14 μsec [Fig. 5(a)]. At 23 μsec, the data on the right array has the same $m = 1$ form as that on the left but rotated counterclockwise about 60° [Fig. 5(b)]. Figure 5(c) depicts data of the twisted equilibrium of a right-handed spheromak. Note that the equilibrium has the same form on the right as on the left, but in this case rotated clockwise 45° (opposite that of the left-handed spheromak). Evidently, the spheromak has relaxed to the minimum energy twisted helical $m = 1$ shape predicted by theory.[11]

IV. ELECTRODE COATINGS

We have also experimented with a number of refractory coatings on the center electrode of the coaxial plasma gun in order to optimize gun performance and spheromak parameters by reducing the impurity level. It is particularly important in the previously described helicity injection experiments that the helicity decay time be maximized ($\tau_K \cong \tau_B/2$); the helicity decay time must be longer than the transit time of the spheromak from gun to tokamak, otherwise little helicity is deposited. In addition, from the standpoint of refueling, impurities are a deleterious addition to the tokamak discharge. The bare steel inner electrode was electroplated with copper, nickel, chromium, and rhodium (0.001–0.002 in. thickness) and was plasma coated with tungsten (0.006 in. thickness). Visible light (230–890 nm) emitted directly from plasma in the gun breech was monitored through an optical fiber in a 1 mm quartz capillary that was immersed in the discharge. In addition, plasma density and temperature and spheromak lifetime were compared for each electrode.

In general, the macroscopic plasma parameters of spheromaks generated with each electrode were roughly the same ($n_e \cong 10^{21}$ m^{-3}, $T_e < 10$ eV, $\tau_{life} \cong 20$ μsec) and the optical spectra from each gun were nearly identical. However, there were a few subtle differences. First, only with the tungsten and chrome electrodes were we able to observe the previously mentioned helicity injection effect. Evidently, small differences in the helicity decay time ($< 10\%$) greatly affect the helicity content of the spheromak that ultimately reaches the tokamak. Second, although most of the hundreds of resolved spectral lines were present for each electrode, some (~ 20) were suppressed for some of the electrodes. For the most part, when suppression of emission of a line was noted (usually an iron, carbon, or nickel line) it was noted on both the tungsten and chrome electrodes. For example, a normally bright CII line (426.7 nm) was strongly suppressed in the tungsten and chrome electrodes. However, there were a few cases when a line was enhanced in the tungsten and chrome electrodes (usually FeI). Third, the quartz capillary eventually (after ~ 30 discharges) became coated with material sputtered from the electrodes. The capillaries used with the tungsten and chrome electrodes had visibly less sputtered material than the others.

V. ACCELERATOR STAGE

Finally, we have designed a new, larger spheromak gun with an acceleration stage similar to that of the Livermore RACE facility.[16] The acceleration stage will provide additional kinetic energy so that the spheromak can be injected into the 1 T magnetic field of the Phaedrus-T tokamak at Wisconsin.[17] The inner and outer electrodes have been increased to 7.6 and 15.2 cm diam, respectively. The gun voltage bank has been increased to 15 kV and will be capable of providing 300 kA of gun current. Special attention has been paid to system cleanliness and high vacuum. The inner and outer electrodes will be fitted with liners that can be heated by the passage of large 60 Hz currents while under vacuum. All of the insulators will be high vacuum compatible ceramic, which should reduce impurities, and electrode surfaces will be coated with refractory metal (tungsten or chromium).

VI. CONCLUSION

In conclusion, a number of recent results of the Caltech spheromak injection experiment have been outlined. First, small spheromaks injected into the ENCORE tokamak have been observed to drive plasma current (via helicity injection) and raise central density. Second, the motion of a spheromak in a toroidal vessel (with and without net toroidal flux) has been measured. Third, a number of electrode materials have been tested. Fourth, a new spheromak gun and accelerator has been designed.

ACKNOWLEDGMENTS

We would like to acknowledge the technical assistance of Frank Cosso and Dave Cutrer. It is a pleasure to acknowledge the suggestions of and useful discussions with J. H. Hammer and C. W. Hartman of Lawrence Livermore National Laboratory and C. W. Barnes, J. C. Fernández, T. R. Jarboe, and I. Henins of the Los Alamos National Laboratory.

This work was supported under U.S. Department of Energy Grant No. DE-FG03-86ER53232.

[1] C. W. Hartman and J. H. Hammer, Phys. Rev. Lett. **48**, 929 (1982).
[2] P. B. Parks, Phys. Rev. Lett. **61**, 1364 (1988).
[3] L. J. Perkins, S. K. Ho, and J. H. Hammer, Nucl. Fusion **28**, 1365 (1988).
[4] H. K. Moffat, *Magnetic Field Generation in Electrically Conducting Fluids* (Cambridge U.P., New York, 1978).
[5] J. B. Taylor, Rev. Mod. Phys. **58**, 741 (1986).
[6] M. R. Brown and P. M. Bellan, to appear in Phys. Rev. Lett.
[7] C. W. Barnes, J. C. Fernández, I. Henins, H. W. Hoida, T. R. Jarboe, S. O. Knox, G. J. Marklin, and K. F. McKenna, Phys. Fluids **29**, 3415 (1986).
[8] T. R. Jarboe, I. Henins, H. W. Hoida, R. K. Linford, J. Marshall, D. A. Platts, and A. R. Sherwood, Phys. Rev. Lett. **45**, 1264 (1980).
[9] J. M. Finn, W. M. Manheimer, and E. Ott, Phys. Fluids **24**, 1336 (1981).
[10] A. Bondeson, G. Marklin, Z. G. An, H. H. Chen, Y. C. Lee, and C. S. Liu, Phys. Fluids **24**, 1682 (1981).
[11] M. J. Schaffer, Phys. Fluids **30**, 160 (1987).
[12] H. Alfvén, L. Lindberg, and P. Mitlid, J. Nucl. Energy, Part C: Plasma Phys. **1**, 116 (1960).
[13] W. C. Turner, G. C. Goldenbaum, E. H. A. Granneman, J. H. Hammer, C. W. Hartman, D. S. Prono, and J. Taska, Phys. Fluids **26**, 1965 (1983).
[14] G. W. Hart, C. Chin-Fatt, A. W. DeSilva, G. C. Goldenbaum, R. Hess, and R. S. Shaw, Phys. Rev. Lett. **51**, 1558 (1983).
[15] S. O. Knox, C. W. Barnes, G. J. Marklin, T. R. Jarboe, I. Henins, H. W. Hoida, and B. L. Wright, Phys. Rev. Lett. **56**, 842 (1986).
[16] J. H. Hammer, C. W. Hartman, J. L. Eddleman, and H. S. McClean, Phys. Rev. Lett. **61**, 2843 (1988).
[17] R. Breun, E. Benck, D. Brouchous, H. Che, D. Diebold, G. Fiksel, R. Fonck, N. Hershkowitz, T. Intrator, M. Kishinevsky, G. Kant, R. Majeski, D. Muller, P. Nonn, J. Pew, P. Probert, J. Sorenson, Y. Wen, and G. Winz, Bull. Am. Phys. Soc. **34**, 1957 (1989).